

Numerical investigation of laser radiation conversion to X rays in experiments with spherical boxes with interior coatings of different materials

S.V. Bondarenko, E.A. Novikova

Abstract. The dynamics of laser and X-ray radiation fields in experiments with spherical boxes was numerically investigated in a sector approximation using the SND-LIRA numerical code. The experiments were performed on the Iskra-5 laser facility at a wavelength $\lambda = 0.657 \mu\text{m}$ (the second harmonic of iodine laser radiation). The characteristics of X-ray generation were investigated with the inner surface of a converter box coated with different- Z materials (Au, Cu, Mg). With lowering Z , the laser energy absorption coefficient k_a decreases and there occurs a lowering of the effective X-ray radiation temperature. Our calculations reveal a strong dependence of the results on the electron free-streaming flux limitation f . In particular, on lowering f from 0.1 to 0.03 for a conventional box with a gold coating, the coefficient k_a decreases from 0.83 to 0.5 and the peak X-ray radiation temperature drops from 170 to 150 eV. In these calculations, the rms nonuniformity of the X-ray irradiation of a capsule with thermonuclear fuel amounted to 1%–3%.

Keywords: X-ray radiation of laser-produced plasma, numerical simulation, spherical converter box.

1. Introduction

As is well known, in indirect-driven laser targets the compression and heating of encapsulated substance to the state at which there occur intense thermonuclear reactions takes place under the action of quasi-equilibrium X-ray radiation, which is generated at the walls of a converter box as a result of absorption of the radiation of a laser driver. In the RFNC–VNIIEF, experiments in the indirect compression of thermonuclear targets have been carried out on the Iskra-5 laser facility since the 1990s. Over a period of several years, a long series of experiments was performed with indirect-irradiation targets using the first harmonic of iodine laser radiation ($\lambda = 1.315 \mu\text{m}$) [1, 2].

S.V. Bondarenko, E.A. Novikova Russian Federal Nuclear Center – The All-Russian Research Institute of Experimental Physics (RFNC – VNIIEF), prosp. Mira, 37, 607190 Sarov, Nizhegorodskaya region, Russia; e-mail: sergvicbond@inbox.ru, bondarenko@otd13.vniief.ru

Received 18 February 2010, revision received 30 March 2010
Kvantovaya Elektronika 40 (5) 406–410 (2010)
Translated by E.N. Ragozin

Subsequently the 12-beam Iskra-5 laser facility was equipped with crystal converters to the second harmonic, which enable carrying out experiments at $\lambda = 0.657 \mu\text{m}$ [3].

In 2008, the Iskra-5 facility was employed to perform a series of experiments at $\lambda = 0.657 \mu\text{m}$ with spherical boxes; the internal surfaces of each of them were coated with different- Z material layers. The objective of these experiments was to investigate the conversion of the laser radiation with this wavelength to X-ray radiation with different- Z materials as well as to study the regime of compression of thermonuclear fuel-filled capsules.

The intent of our work is the numerical investigation of the dynamics of laser and X-ray radiation fields in spherical boxes with gold, copper, and magnesium coatings of the interior surface in experiments involving the second harmonic of iodine laser radiation. In these simulations we determined the conditions of laser radiation absorption at the box walls, found the spectra of the nonequilibrium X-ray radiation generated in the spherical boxes, and calculated the nonuniformity of the X-ray irradiation of the thermonuclear fuel capsule.

These simulations were performed using the SND-LIRA numerical technique [4, 5], which enables calculating – in the framework of a sector approximation in the three-dimensional formulation of the problem – the propagation and absorption of laser radiation as well as the generation and transfer of X-ray radiation in the interior volume of a converter box.

2. Formulation of the problem

At the present time the Iskra-5 facility permits conducting experiments with 12 beams with a total laser energy of 2–3 kJ delivered to the target for a subnanosecond duration of a laser pulse at a wavelength $\lambda = 0.657 \mu\text{m}$. The beams are injected into the interior volume of a spherical converter box 1.6 mm in diameter via 6 openings 400 μm in diameter. In all calculations the energy of laser radiation was assumed to be $E_{\text{las}} = 2.45 \text{kJ}$ for a half-height pulse duration $\tau_{0.5} = 0.6 \text{ns}$. At the second harmonic, the parameters of the focusing optics were changed: in particular, for a focal length $F = 1600 \text{mm}$, the beam diameter was $D = 300 \text{mm}$ (previously, at the first harmonic, for $F = 1100 \text{mm}$ the beam diameter D was equal to 680 mm). In these conditions, the primary laser spots on the interior surface of the spherical box occupy approximately 8% of its surface. Consequently, the experiments involving the second harmonic of iodine laser radiation are charac-

terised by a high degree of anisotropy of heating of the box walls by laser radiation.

One-dimensional numerical simulations turn out to be inadequate in this case, because they do not permit taking into account the nonuniform character of the heating of box wall substances and the anisotropy of the field of non-equilibrium X-ray radiation in the interior box volume. This task may be solved in the framework of the sector approximation employed in the SND-LIRA numerical code [4, 5]. In the calculation of radiation field dynamics, the surface of the spherical box was divided into gas-dynamically independent domains (sectors) in such a way that a separate sector was allocated to every primary laser spot (sector Nos 2–13). The box wall experiences a strong heating in the regions of laser spots as a consequence of absorption of the high-intensity laser radiation, resulting in the violation of the spherical symmetry of the gas-dynamic motion in these regions. A plane gas-dynamic problem was numerically solved in order to model the intense substance expansion in the sectors. The remaining part of the interior surface was united into sector No. 1, in which the geometry was assumed to be spherical.

One-dimensional calculations were performed by the SND code [6] in each sector. The following physical processes were taken into account: the plasma motion in a two-temperature approximation, electron and ion heat conductivities with electron–ion relaxation, the transfer of X-ray radiation in a spectral multigroup diffusion approximation (100 spectral groups evenly distributed over the 0–5 keV interval). The ionisation kinetics and population densities of different atomic and ionic states were calculated by the average ion model [7] with the inclusion of the splitting of atomic and ionic energy states in orbital quantum number (l -splitting) [8]. At laser radiation intensities of $\sim 10^{15} \text{ W cm}^{-2}$ achieved in primary laser spots, the effects of electron heat flux limitation makes themselves strongly evident, and so in our simulations we used two different values of the flux limitation f : 0.1 and 0.03.

Therefore, the plasma state at the walls of converter box is found from one-dimensional numerical (sector) calculations. Furthermore, in the SND-LIRA code the three-dimensional algorithms of laser and X-ray radiation transfer are used. Combining these approaches in the framework of one numerical technique permits carrying out the numerical simulations of the three-dimensional designs of converter boxes for indirect-irradiation targets. The X-ray radiation transfer in the SND-LIRA code is calculated by the method of viewing angles with the calculation of visibility integrals by the Monte-Carlo method [9]. Every laser beam was defined as a statistical ensemble of individual beams propagating independently according to the laws of geometrical optics. This determined the spatial and angular characteristics of the laser radiation beams injected into the spherical box through the openings. The spatial structure of laser irradiation was also calculated using the Monte-Carlo approach by summing up the contributions of individual beams. The absorption of laser radiation (by the inverse bremsstrahlung mechanism) was calculated for the temperature and density distributions in the near-wall plasma obtained by way of one-dimensional (sector) simulations. In this case, a part of the laser radiation flux experienced specular reflection from the interior box surface and then arrived at the walls of the converter box again or escaped through the openings. A similar numerical code was

developed for interpreting the experiments on the indirect target irradiation with a spherical box carried out on the OMEGA laser facility [10].

3. Results of calculations

Using the SND-LIRA code, we performed a series of modelling of the dynamics of laser and X-ray radiation fields in experiments involving spherical boxes with coatings of different materials deposited on the interior box surfaces: a $\sim 1\text{-}\mu\text{m}$ -thick gold layer, a $\sim 2\text{-}\mu\text{m}$ -thick layer of copper, or a $4\text{-}\mu\text{m}$ -thick magnesium layer. For the specified thicknesses, the layers of these materials do not burn through in the course of laser heating and the X-ray radiation spectrum inside the box is unaffected by the material of the substrate on which the coating was deposited. Figure 1 shows the structure of laser irradiation of the interior surface of the spherical box with the use of the second harmonic of iodine laser radiation ($\lambda = 0.657 \mu\text{m}$). The regions of primary laser irradiation stand out sharply against the background of this structure.

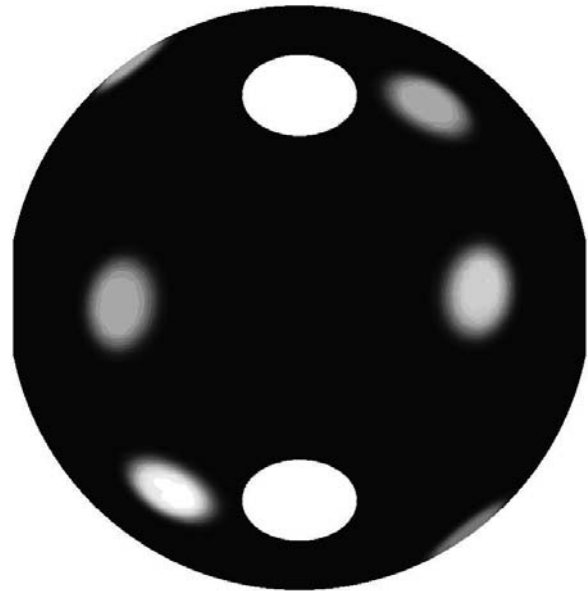


Figure 1. Structure of laser irradiation of the interior surface of a spherical box in experiments involving the second harmonic of iodine laser radiation ($\lambda = 0.657 \mu\text{m}$).

The concentrated action of laser radiation produces strong electron temperature gradients in the near-wall plasma. For the purpose of describing heat transfer in the hot and rarefied plasma, one cannot take advantage of the classical relationship derived by Spitzer [11] under the assumption that the electron free path is much shorter than the characteristic temperature gradient scale length. To avoid an unphysical situation, Malone et al. [12] came up with the idea of limiting the heat flux transferred by electrons by the limiting value $q = f k T_e v_e$ (T_e is the electron temperature, k is the Boltzmann constant, and v_e is the thermal electron velocity) with $f \sim 0.65$. It turned out that the flux limiter had to be lowered to $0.03 \leq f \leq 0.1$ (see, for instance, Shvarts et al. [13] and references therein) in order to bring simulations in line with experimental data. Substantiating the necessity to employ the values of f which are

smaller by an order of magnitude calls for the kinetic treatment of the electron heat transfer in rarefied hot plasmas [13, 14].

The results of several simulations for two values of the flux limiter f are collected in Table 1. For $f = 0.1$, the effects of limitation appear only slightly. In this case, the major fraction of laser radiation is absorbed in the primary spots. For intensities of $\sim 10^{15} \text{ W cm}^{-2}$, the coefficient of laser radiation absorption observed experimentally for a gold target is possible to reproduce in simulations for $f \approx 0.03$. As suggested by the data of Table 1, for $f = 0.03$ the absorption of laser radiation in the primary spots turns out to be much lower (for the gold coating, in particular, the absorption coefficient k_a lowers from 0.83 to 0.50), while the loss of laser energy through the openings is substantially higher. The laser radiation which is not absorbed in the primary spots experiences specular reflection from the interior box surface and is either incident on it again or is scattered through the openings.

Table 1. Plasma parameters calculated for different values of the electron heat flux limiter.

Coating material	$T_{X\max}/\text{eV}$		k_a		δ (%)	
	f	f	f	f	f	f
Au	248	192	0.83	0.50	3.5	19
Cu	220	160	0.72	0.39	6.6	26
Mg	178	127	0.59	0.30	13	35

Note: f is the electron heat flux limiter; $T_{X\max}$, k_a are the peak temperature of X-ray radiation in the primary spots and the coefficient of laser radiation absorption in the primary spots; δ is the fraction of laser energy scattered through the openings.

Figure 2 shows the temperatures of X-ray radiation in the interior box volume obtained for the two values of f specified above. One can see that for $f = 0.03$ the temperatures are substantially lower. (In the gold coated box, in particular, for $f = 0.1$ the radiation temperature is $T_X \approx 170 \text{ eV}$ as compared to 150 eV for $f = 0.03$.) Furthermore, the peak of radiation temperature (which corresponds to the moment the luminosity of box walls under the action of a laser pulse reaches its peak) is less pronounced against the background of the subsequent

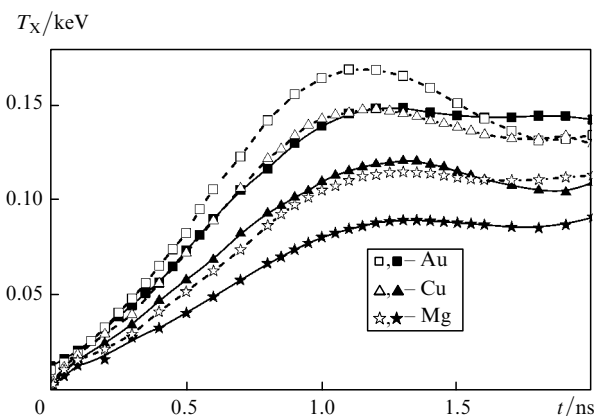


Figure 2. Effective temperature of X-ray radiation for $f = 0.1$ (empty marks) and $f = 0.03$ (full marks) at different points in time. The data are given for spherical boxes with coatings of gold, copper, and magnesium.

substance heating arising from the collisions of the streams of plasma evaporated from the box walls and the capsule surface. With reference to the data of Fig. 2, the efficiency of laser radiation conversion to X-rays lowers with decreasing the atomic number of the substance coating the box walls.

Figure 3 shows the spectral characteristics of X-ray radiation at the surfaces of standard capsules $280 \mu\text{m}$ in diameter located at the centre of spherical boxes with gold, copper, and magnesium coatings of the interior surface. The calculated data correspond to the moment the luminosity of box walls reaches its peak. The X-ray spectra contain spectral lines characteristic of the specified substances in the conditions under consideration. In particular, in the case of the gold-coated box one can see the M band in the short-

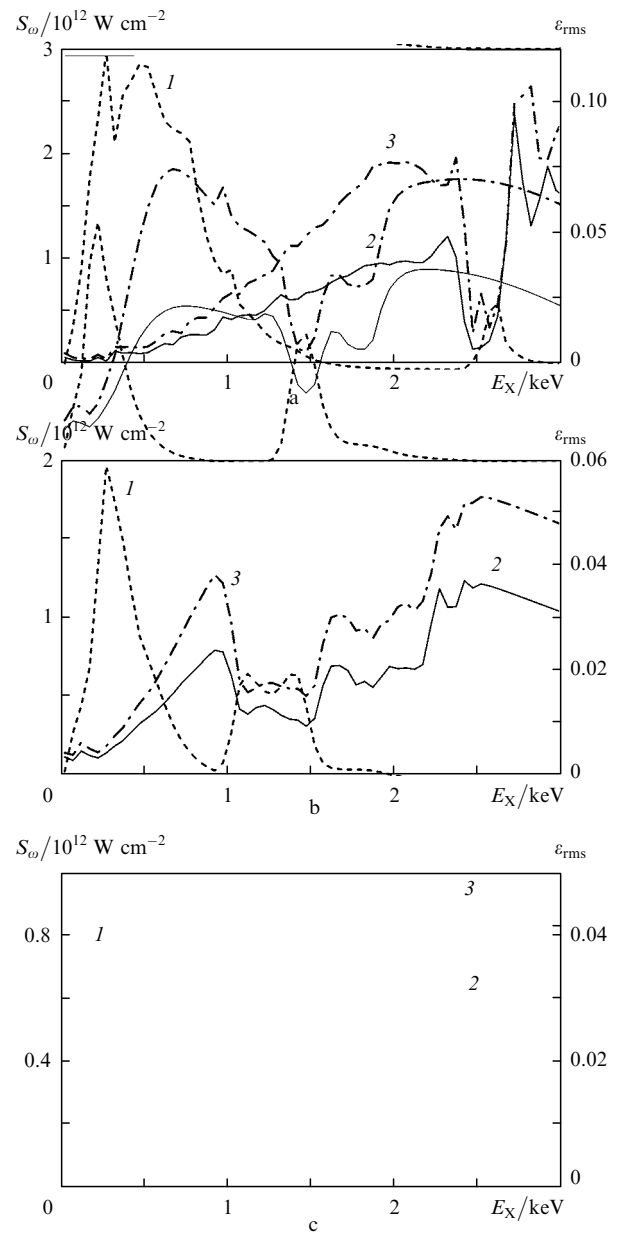


Figure 3. Calculated characteristics of the X-ray radiation field in the interior volumes of spherical boxes with coatings of gold (a), copper (b), and magnesium (c): (1) spectral X-ray irradiation flux at the surface of a capsule $280 \mu\text{m}$ in diameter; (2, 3) rms nonuniformities of the X-ray capsule irradiation for laser beams of equal energy and with the inclusion of an rms energy scatter of about 20 %, respectively.

wavelength part of the spectrum for photon energies $E_X = 2.5 - 3$ keV; seen in the case of the copper-coated box is the relatively short-wavelength *L* band for $E_X = 1.0 - 1.5$ keV; observed in the wall radiation of the magnesium-coated box is the *K* band at energies $E_X \approx 1.5$ keV.

Figure 3 also shows the rms nonuniformities ε_{rms} of the X-ray capsule illumination in different spectral groups in the case of idealised laser illumination (when the energies of all 12 beams are equal) and for an rms energy spread of $\sim 20\%$. All data pertain to the simulations with $f = 0.03$ and are given for the instant of the highest luminosity of the box walls. For the gold coating, $f = 0.03$ proves, in our opinion, to be more adequate to the experimental situation under consideration.

As is clear from the data presented, there occurs a substantial reduction of ε_{rms} in the spectral region where the X-ray radiation intensity is rather high. This parameter is found to be minimal in the relatively long-wavelength part of the spectrum: for all coatings under consideration, for $E_X \leq 1$ keV the nonuniformity of capsule irradiation is equal to $\sim 1\%$. In the gold-coated box, the nonuniformity ε_{rms} in the range of the *M* band for $E_X = 2.4 - 2.6$ keV also amounts to $\sim 1\%$. Furthermore, in the short-wavelength lines (for $E_X = 1.0 - 1.5$ keV in the copper-coated box and in the range of the *K* band in the magnesium-coated box for the same value of E_X) the nonuniformity of capsule irradiation also lowers and amounts to $1.5\% - 2\%$. In the remaining part of the spectrum, the rms nonuniformity of capsule irradiation may be as high as $5\% - 10\%$.

Table 2 gives the spectrum-integrated rms nonuniformities of the X-ray capsule irradiation at the moment the luminosity of box wall reaches its peak. As these data suggest, for $f = 0.1$ the nonuniformity is equal to $2\% - 3\%$ for beams of equal energy and rises to $3\% - 5\%$ in the case of their $\sim 20\%$ energy spread. For $f = 0.03$ there occurs a substantial redistribution of laser energy due to the low absorption in the primary spots, resulting in a higher spatial uniformity of the X-ray source at the box walls. In this case, the X-ray irradiation of the capsule surface is more uniform ($\varepsilon_{\text{rms}} = 1\% - 2\%$).

Also given in Table 2 are the values of ε_n , which characterise different spatial scales inherent in the nonuniform structure of capsule X-ray irradiation [5] (n is the number of a spherical harmonic). The ‘partial’ nonuniformities ε_n are related to the rms nonuniformity by the following simple relation:

$$\varepsilon_{\text{rms}} = \sqrt{\sum_{n=1}^{\infty} \varepsilon_n^2}.$$

This relation is a consequence of the completeness of the system of normalised spherical harmonics. One can see

from Table 2 that the capsule irradiation nonuniformity is associated with low-order harmonics ($n = 1 - 4$), because small-scale nonuniformities are effectively smoothed out in the transfer of X-ray radiation from the box walls to the capsule surface.

It is noteworthy that the resultant data exhibit a strong dependence of the computational result on the flux limiter f . The conditions in the primary spots (recall that they occupy only about 8% of the interior box surface for the scheme of laser target irradiation existing on the Iskra-5 facility) turn out to be critically important, and the simulation uncertainty in these local regions is responsible for the uncertainty of the description of X-ray radiation generation in the entire volume of a converter box. Unfortunately, the data available from the literature (for instance, the data on the absorption of laser radiation with different wavelengths) do not permit the value of the flux limiter f to be unambiguously selected for all materials that coat the walls of spherical converter boxes involved in experiments on the Iskra-5 laser facility. The high laser irradiation intensities ($\sim 10^{15}$ W cm $^{-2}$) serve to produce in these regions the hot nonequilibrium plasma with a moderate optical thickness of the radiating layer. According to the resultant computational data, this gives rise to a strong angular dependence of the luminosity of the heated layer, i.e. to a substantial anisotropy of the X-ray radiation source in the region of primary laser spots.

4. Conclusions

We have performed numerical simulations of the dynamics of radiation fields in experiments involving spherical boxes with different interior surface coating materials on the Iskra-5 laser facility (a wavelength $\lambda = 0.657$ μm). The computational results show that the laser energy absorption coefficient k_a and the effective temperature of laser radiation in the box exhibit a sharp decrease with decreasing the atomic number Z of the material coating the box walls (in going from a gold coating to copper and magnesium coatings).

Our simulations emphasise the importance of adequate description of electron heat transfer in the box. In the simulation of these experiments, the electron heat flux limiter f (defines the maximum fraction of the total kinetic energy flux which may be transferred by electrons) turns out to be the critical parameter. The values $0.03 \leq f \leq 0.1$ are commonly accepted in the simulation of laser experimental conditions, when strong temperature gradients are inherent in the plasma.

The simulations were carried out for the two values of f that limit the specified range. For $f = 0.03$ there occurs ‘imprisonment’ of heat in the interior box volume accessible

Table 2. Calculated partial nonuniformities ε_n of the X-ray capsule irradiation at the moment the luminosity of box walls reaches its maximum for a 20% spread of laser beams in energy.

Coating material	$\varepsilon_{\text{rms}}(\%)$		$\varepsilon_{\text{rms}}^{\text{D}}(\%)$		$\varepsilon_1(\%)$		$\varepsilon_2(\%)$		$\varepsilon_3(\%)$		$\varepsilon_4(\%)$	
	f		f		f		f		f		f	
	0.1	0.3	0.1	0.3	0.1	0.3	0.1	0.3	0.1	0.3	0.1	0.3
Au	2.1	1.0	3.3	1.6	1.5	0.74	2.2	1.1	1.8	0.89	0.28	0.22
Cu	2.4	1.1	3.4	1.4	1.4	0.64	2.2	0.98	2.1	0.81	0.26	0.20
Mg	2.8	1.3	4.4	2.0	2.0	0.92	2.8	1.2	2.6	1.2	0.25	0.19

Note: ε_{rms} is the rms nonuniformity of the irradiation of a capsule 280 μm in diameter for equal beam energies; $\varepsilon_{\text{rms}}^{\text{D}}$ is the capsule irradiation nonuniformity with accounting for beam energy disbalance.

for the propagation of laser radiation. This circumstance has two implications. First, the plasma heating lowers the coefficient of laser radiation absorption. Second, the limitation of heat transfer to the more dense layers of the above-critical plasma lowers the temperature of the X-ray radiation generated at the box walls. For a conventional box with a gold coating, in particular, lowering f from 0.1 to 0.03 decreases the coefficient k_a of absorption by the spots of primary laser irradiation from 0.83 to 0.50, and the peak X-ray radiation temperature $T_{X\max}$ in the box falls from 170 eV to 150 eV.

The spectral rms nonuniformity of the X-ray radiation flux at the surface of a thermonuclear fuel capsule was calculated. For the target design in use and the configuration of laser beams existing on the Iskra-5 facility, the spectrum-integrated nonuniformity of X-ray capsule irradiation is equal to 1%–3%.

References

1. Abzaev F.M., Bel'kov S.A., Bessarab A.V., et al. *Zh. Eksp. Teor. Fiz.*, **114**, 155 (1998).
2. Abzaev F.M., Bessarab A.V., Bel'kov S.A., et al. *Zh. Eksp. Teor. Fiz.*, **114**, 1993 (1998).
3. Annenkov V.I., Bel'kov S.A., Bessarab A.V., et al., in *Tez. Dokl. Mezhdunar. Konf. 'Zababakhinskie Nauchnye Chteniya'* (Abstracts of the Intern. Conf. 'Zababakhin Scientific Readings') (Snezhinsk, 2007) p. 107.
4. Bondarenko S.V., Dolgoleva G.V., Novikova E.A. *Voprosy Atomnoi Nauki i Tekhniki. Ser. Matematicheskoe Modelirovanie Fizicheskikh Protseessov*, (3-4), 15 (2007).
5. Bondarenko S.V., Dolgoleva G.V., Novikova E.A. *Kvantovaya Elektron.*, **37** (4), 372 (2007) [*Quantum Electron.*, **37** (4), 372 (2007)].
6. Dolgoleva G.V. *Voprosy Atomnoi Nauki i Tekhniki. Ser. Metodiki i Programmy Chislennogo Resheniya Zadach Matematicheskoi Fiziki*, (21), 29 (1983).
7. Bel'kov S.A., Dolgoleva G.V. *Voprosy Atomnoi Nauki i Tekhniki. Ser. Matematicheskoe Modelirovanie Fizicheskikh Protseessov*, (1), 59 (1992).
8. Bel'kov S.A., Gasparyan P.D., Kochubei Yu.K., Mitrofanov E.I. *Zh. Eksp. Teor. Fiz.*, **111**, 496 (1997).
9. Sobol' I.M. *Chislennyye Metody Monte-Karlo* (Numerical Monte-Carlo Methods) (Moscow: Nauka, 1973).
10. Shnittman J.D., Craxton R.S. *Phys. Plasmas*, **7** (7), 2964 (2000).
11. Spitzer L., Harm R. *Phys. Rev.*, **89**, 977 (1953).
12. Malone R.C., McCrory R.L., Morse R.L. *Phys. Rev. Lett.*, **34**, 721 (1975).
13. Shvarts D., Delettrez J., McCrory R.L., Verdon C.P. *Phys. Rev. Lett.*, **47** (4), 247 (1981).
14. Silin V.P. *Zh. Eksp. Teor. Fiz.*, **106**, 1398 (1994).